

submitted to ApJLett

High frequency oscillations in outbursts of Kerr-metric slim disks

Li Xue^{1,2}

Department of Astronomy and Institute of Theoretical Physics and Astrophysics, Xiamen University, Xiamen, Fujian 361005, China

lixue@xmu.edu.cn

Włodek Kluźniak²

Copernicus Astronomical Center, ul. Bartycka 18, PL-00-716 Warszawa, Poland

wlodek@camk.edu.pl

Aleksander Sądowski

Harvard-Smithsonian Center for Astrophysics, 60 Garden St., Cambridge, MA 02134, USA

asadowski@cfa.harvard.edu

Ju-Fu Lu

Department of Astronomy and Institute of Theoretical Physics and Astrophysics, Xiamen University, Xiamen, Fujian 361005, China

lujf@xmu.edu.cn

and

Marek Abramowicz^{1,2}

Physics Department, Gothenburg University, SE-412-96 Göteborg, Sweden

marek.abramowicz@physics.gu.se

ABSTRACT

¹Copernicus Astronomical Center, ul. Bartycka 18, PL-00-716 Warszawa, Poland

²Institute of Physics, Faculty of Philosophy and Science, Silesian University in Opava, Bezručovo nám. 13 CZ-746-01 Opava, Czech Republic

We numerically investigate the thermally unstable accretion disks around black holes. We adopt an evolutionary viscous stress equation to replace the standard alpha-prescription based on the results of two MHD simulations. We find a kind of interesting oscillations on some running models in limit-cycle outburst state. The oscillations arise near the inner boundary and propagate radially outwards. We deem that they are the trapped p -mode oscillations excited by sonic-point instability. We directly integrate the local radiation cooling fluxes to construct the mimic bolometric light-curve. We find a series of overtones beside the fundamental harmonic on the power spectra of mimic light-curves. The frequency of the fundamental harmonic is very close to the maximum epicyclic frequency of the disk and the frequency ratio of the fundamental harmonic and overtones is a regular integer series. We suggest that the code for ray-tracing calculation must be time-dependent in virtual observation and point out the robustness of the black hole spin measurement with high frequency QPOs.

Subject headings: accretion, accretion disks — black hole physics — gravitation — relativistic processes — X-rays: bursts

1. Introduction

High-frequency quasi-periodic oscillations (HFQPOs) have been observed in some black hole (BH) X-ray binaries, which only appear in "steep power law" state in high luminosity ($L > 0.1L_{\text{Edd}}$) and are in range of 40 to 450Hz. These frequencies are comparable to the orbital frequency of innermost stable circular orbit (ISCO) of a stellar-mass BH. It is believed that the mechanism behind them is closely related to the dynamics of inner regions of BH accretion disks (see Remillard & McClintock 2006; Kato et al 2008; Belloni et al 2012, for reviews).

The pioneering work of Kato (1978) studied the effect of viscosity on the disk stability and found the sonic-point instability (its original name is pulsational instability), which is the excitation process of so called p -mode oscillations in transonic accretion flows (this oscillation has the other name, inertial-acoustic oscillation, but we only call it p -mode oscillation in this paper). The mechanism of this instability is analogous to the ϵ -mechanism in stellar pulsations. If the viscous parameter α of α -prescription (Shakura & Sunyaev 1973) is larger than a critical value, the instability will arise from the phase relation between the viscous heat generation and oscillation, i.e. the viscous heat generation increase (decrease) in the compressed (expanded) phase of disk oscillation (Kato 1978; Kato et al 1988).

A series of works (Matsumoto et al 1988, 1989; Chen & Taam 1995; Miranda et al 2014) were dedicated to study the role of viscosity on HFQPOs. They all found the oscillation, whose frequency is close to the maximum of epicyclic frequency κ_{\max} . Additionally, Miranda et al (2014) also found many overtones, whose frequencies are close to the integer multiples of κ_{\max} .

Though the famous α -prescription has been used extensively since 1973, it may be too simple to closely accord with actual accretion flows. The magnetohydrodynamic (MHD) shearing box simulations of Hirose et al (2009) implied that there is certain time-delay between the viscous stress and total pressure instead of the instantaneity introduced by α -prescription. The other work of Penna et al (2013), which is based on a few relativistic MHD global simulations, pointed out that the parameter α is a function of radius but not constant in the inner disk region. More than one decade ago, Yamasaki & Kato (1996) analyzed effects of viscous time-delay on the p -mode oscillations and they found that it has a little of inhibition on the growth of oscillations but excitation still exists for high viscosity cases.

Our work presented in this letter is also dedicated to study the role of viscosity on QPOs. The distinction of our model is the evolutionary viscous stress equation (instead of the α -prescription), which is constructed to mimic effects of viscous time-delay and inconstant α basing on the results of Hirose et al (2009) and Penna et al (2013).

2. Equations

In this letter, we consider the axisymmetric relativistic accretion flows around black holes. The Boyer-Lindquist coordinates t, r, θ, ϕ are used to describe the space-time. The governing equations of accretion flows are written as following,

$$\frac{\partial \Sigma}{\partial t} = -\frac{r\Delta^{1/2}}{\gamma A^{1/2}} \left[\Sigma \frac{\partial u^t}{\partial t} + \frac{1}{r} \frac{\partial}{\partial r} \left(r \Sigma \frac{V}{\sqrt{1-V^2}} \frac{\Delta^{1/2}}{r} \right) \right], \quad (1)$$

$$\frac{\partial V}{\partial t} = \frac{\sqrt{1-V^2}\Delta}{\gamma A^{1/2}} \left[-\frac{V}{1-V^2} \frac{\partial V}{\partial r} + \frac{\mathcal{A}}{r} - \frac{1-V^2}{\rho} \frac{\partial p}{\partial r} \right], \quad (2)$$

$$\frac{\partial \mathcal{L}}{\partial t} = -\frac{\Delta}{\gamma A^{1/2}} \frac{V}{\sqrt{1-V^2}} \frac{\partial \mathcal{L}}{\partial r} - \frac{\Delta^{1/2}}{\gamma A^{1/2} \Sigma} \frac{\partial}{\partial r} \left(\frac{2\Delta}{r} S_{r\phi} \right), \quad (3)$$

$$\frac{\partial H}{\partial t} = -\frac{UH}{r} - \frac{1}{\gamma} \frac{V}{\sqrt{1-V^2}} \frac{\partial H}{\partial r}, \quad (4)$$

$$\frac{\partial U}{\partial t} = \frac{\Delta^{1/2} r}{\gamma^2 A^{1/2} H} \mathcal{R} - \frac{U}{\gamma^2} \left(\frac{V}{(1-V^2)^2} \frac{\partial V}{\partial t} + \frac{\mathcal{L} r^2}{A} \frac{\partial \mathcal{L}}{\partial t} \right)$$

$$-\frac{U}{H} \frac{\partial H}{\partial t}, \quad (5)$$

$$\frac{\partial T}{\partial t} = \frac{1}{\Sigma} \frac{r \Delta^{1/2}}{\gamma A^{1/2}} \left[\frac{F^+ - F^-}{c_V} + (\Gamma_3 - 1) T \Sigma \left(-\frac{\partial u^t}{\partial t} - \frac{1}{r^2} \frac{\partial}{\partial r} (r^2 u^r) \right) \right] - \frac{V \Delta}{\gamma \sqrt{1 - V^2} A^{1/2}} \frac{\partial T}{\partial r}. \quad (6)$$

Where Σ , V , \mathcal{L} , H , U , T , and $S_{r\phi}$ are the surface density, radial velocity (measured in the corotating frame), angular momentum per unit mass ($\mathcal{L} \equiv u_\phi$), half thickness of disk, vertical velocity of the surface, local temperature of accreted gas, and viscous stress (only $r\phi$ -component is non-vanishing), respectively. These equations are all derived from the conservation of the stress-energy tensor, and almost the same as those in our previous paper Xue et al (2011) (see that paper for the detailed derivations as well as definitions of γ , A , Δ , and etc).

As mentioned in previous section, we adopt an additional evolutionary stress equation to describe the viscosity instead of the α -prescription. This equation can be written as

$$n\tau^* \frac{\partial S_{r\phi}}{\partial t} = S_{r\phi}^* - S_{r\phi}, \quad (7)$$

where the factor $n\tau^*$ is the practical viscous time-delay, which is scaled with the typical delay τ^* by parameter n ; $S_{r\phi}^*$ is the expected stress by turbulence. The definitions of τ^* and $S_{r\phi}^*$ can be written as

$$\tau^* = - \left(\frac{\gamma^2 A \Omega}{r^4} \frac{\partial \ln \Omega}{\partial \ln r} \right)^{-1}, \quad (8)$$

$$S_{r\phi}^* = - \frac{\nu \Sigma A^{3/2} \gamma^3}{2r^3 \Delta^{1/2}} \frac{\partial \Omega}{\partial r}, \quad (9)$$

where

$$\Omega = \frac{d\phi}{dt}, \quad (10)$$

$$\nu = \frac{2}{3} \alpha H \sqrt{\frac{p}{\rho}}, \quad (11)$$

$$\alpha = \alpha_0 \left(\frac{1 - 2Mr^{-1} + a^2 r^{-2}}{1 - 3Mr^{-1} + 2aM^{1/2} r^{-3/2}} \right)^6. \quad (12)$$

If $\alpha = \text{const}$ and $n \rightarrow 0$, equation (7) will reduce to $S_{r\phi} = S_{r\phi}^*$, which is the same as the α -prescription in Xue et al (2011). It means that equation (7) contains the α -prescription as a trivial case. Equation (12) determines the dependence of α on radius r , BH mass M and spin a . The radial factor, including the exponent 6, was suggested by Penna et al (2013). Under

this profile, α is almost a constant α_0 in outer disk region with large r and increases to higher value radially inwards. We set $\alpha_0 = 0.1$ and fix the mass supplying rate $\dot{M}_{\text{out}} = 0.06\dot{M}_{\text{Edd}}$ (see table 1 for the definition of Eddington accretion rate, \dot{M}_{Edd}) at the outer boundary in this work. In practice, these settings are sufficient to make the disk thermally unstable and we indeed observe the limit-cycle outburst from running code.

After defining $S_{r\phi}$, the viscous heating rate F^+ in equation (6) is redefined as

$$F^+ = -2\frac{\gamma A^{1/2} \Delta^{1/2}}{r^3} \frac{\partial \Omega}{\partial r} \cdot S_{r\phi}, \quad (13)$$

which would be reduced to the one in Xue et al (2011) when $n \rightarrow 0$.

3. Instabilities

We update our previous code established in Xue et al (2011) and run it for eleven numerical models, whose parameters are listed in table 1. Lin et al (2011) and Ciesielski et al (2012) studied the impact of viscous time-delay on the thermal instability and found that it is not remarkable for small enough time-delay. Indeed, we observe the expected limit-cycle outbursts on all models with the time delay parameters n in the range 0 to 4. Therefore, the time-delay implemented in our code does not affect the limit-cycle outbursts.

Among these models, S8 and S30 are two typical ones. S8 is a disk around a non-spinning black hole as well as S30 around a fast-spinning one. In figure 1, we show the bolometric light curves for these two models respectively. For each point on light-curves, the disk luminosity is made by integrating the local radiation cooling fluxes, and the sampling time corresponds to the frequency 10^4Hz , which is enough to reveal any harmonic with frequency lower than $5 \times 10^3\text{Hz}$ in the power spectral density (PSD). Due to the difficulties in hydrodynamical calculation, we only obtain one outburst light curve for S8 and 0.7s-long luminosity ascending light curve for S30. However, they are long enough for the calculation of PSDs. In figure 2, we show the relevant PSDs for S8 and S30. The fundamental frequency (the lowest frequency of harmonics) is $\sim 74.9\text{Hz}$ for S8 and $\sim 285.6\text{Hz}$ for S30, which are both close to 71.3Hz and 300Hz , the respective maximal epicyclic frequencies, which are also the maximum predicted frequencies of axisymmetric oscillations in the trapped p -mode theory (see Kato 2001; Kato et al 2008, and a detailed relativistic analysis is ongoing by our colleague Jiří Horák). The spectrum of axisymmetric ($m = 0$), horizontal p -modes was recently computed by Giussani et al (2014), who show that in addition to a discrete set of lower frequency modes which are trapped in the inner disk, there are modes of frequency very close to the maximal epicyclic frequency in which the oscillation is transmitted to the

outer disk. In table 1, we also list the fundamental frequencies observed from the other oscillating models, which are all close to the theoretical values though they vary in a narrow frequency range.

In figure 3, we show an oscillating cycle of model S8 for V (upper two panels) and $S_{r\phi}$ (lower two panels). The oscillations arise near the inner boundary and propagate outwards. In the figure, one can follow the motion of individual wavelets. The negative V denotes inflow and negative gradient of V corresponds to the compression (inflow speed of inner is slower than outer) as well as positive gradient to the expansion (inflow speed of inner is faster than outer). Thus, any wavelet on the V -profiles can be divided into the compressed wave-front and expanded wave-rear regions. For example, the left-most wavelet on initial V -profile (red curve in the upper-left panel) can be divided into the wave-front (between dashed and dash-dotted lines) and wave-rear (between solid and dashed lines) regions. The relevant variation of $S_{r\phi}$, which is proportional to the viscous heating, is showed in the lower-left panel. $S_{r\phi}$ (as well as the viscous heating) monotonously increases in compressed wave-front (see the red curve between dashed and dash-dotted lines) but it unceasingly increases after the maximal compression (takes place at the dashed line) and then decreases in the expanded wave-rear. This non-monotonicity of $S_{r\phi}$ in wave-rear is due to the time-delay contained by equation 7. We deem that this is the phase relation between the viscous heat generation and disk oscillation, which implies the arise of sonic-point instability for p -mode oscillation (Kato 1978; Kato et al 1988). Thus, we also deem that the oscillations actually arise near the sonic-point, which is included in our computational domain and very close to the inner boundary.

4. Results and Discussions

In table 1, there are the other nine models with different viscous settings but with the same BH mass, BH spin and mass supply rate (fixed accretion rate at the outer boundary) as S8. We only observe oscillations on the models with non-vanishing delay and large enough constant α ($\gtrsim 0.3$) or α -profile. In fact, the effective value on the α -profile increases inwards from constant 0.1 in outer disk region to the maximum 0.45 at the inner boundary. Thus, the impact of α -profile is similar to the large constant α while it just becomes large enough near the origin of instability, sonic-point. The facts of these oscillating models imply that the large α (at least near sonic-point) is a necessary condition for the arise of sonic-point instability as well as p -mode oscillation, which is consistent with the analysis of Kato et al (1988) and Yamasaki & Kato (1996).

On the other view, we note the effect of delay on the appearance of oscillations. The

oscillating models with $n = 1$ (S7 and S8) have the oscillations during the whole outburst. The other oscillating models with $n \neq 1$ (S1, S2 and S17) lose the oscillations in different luminosity stages. The models with $n = 0$ (S3, S4, and S16) have no any oscillation though they have large enough α , while the disappearance of the oscillations on models S5 and S15 is due to the small α . These facts imply that τ^* may be a favorable delay for oscillation excitation on the disk around a $10M_\odot$ Schwarzschild BH under the large α . The last model in table 1, S30 is a special case for a fast-spinning Kerr BH, which has another favorable delay $4\tau^*$. This may imply the dependence between the viscous time-delay and BH spin.

Focusing on the luminosity of the oscillating models, we observe oscillations only in the limit-cycle outburst state ($L \gtrsim 0.2L_{\text{Edd}}$) when the inner disk region has switched to slim disk mode. On the contrary, there is no any oscillation observed in the limit-cycle quiet state ($L \sim 0.01L_{\text{Edd}}$). This is consistent with the HFQPO observations, but cannot be compared with the sonic-point instability theory which does not discriminate between accretion rates. Recently, the shearing box simulation of Hirose et al (2014) implied that the effective α is enhanced by the vertical convection during the outburst, which is similar to the conception of Milsom et al (1994). Thus, larger α required by the p -mode oscillation may be caused by the outburst, explaining why HFQPOs are observed only in high luminosity state.

Beside the fundamental harmonic, there are many overtones in both of the two spectra in figure 2. The frequency ratio of fundamental harmonic and its overtones is a regular integer series, which is also observed by Miranda et al (2014) in their 2D-simulations (in radial and azimuthal dimensions) when the axisymmetric p -mode become dominant for large α . However, no overtones are observed by Chen & Taam (1995). Perhaps, this is due to their adopting of the viscous prescription with $S_{r\phi} \propto p_{\text{gas}}$ instead of $S_{r\phi} \propto p_{\text{total}}$ in Miranda et al (2014) and our models. These interesting overtones may be potentially useful for explaining the observational QPO pairs, which are always in a specific integer frequency ratio.

Subsequently, the virtual observation from our numerical results will be logical and interesting. However, it would require more careful treatment. For example, the effective time-delay of arrival caused by the gravitational bending on the trajectories of emitted photons and the large observational view-angle, and effective blocking caused by the gravitational red-shift and the other shields.

As a rough evaluation for the effective time-delay of arrival, one can consider the observation from an almost edge-on disk, on which the photons emitted from two locations apart from distant $\Delta r = 203M$ at the same observer's time (t) will arrive at the observer with the rough delay $\Delta t = 0.01\text{s}$ comparable with the period of 71.3Hz (our results presented in figures 1 and 2 can be roughly regarded as from the face-on disks). The distant $\Delta r = 203M$ is comparable with the radius of outward wavelets propagating area, so it is possible to change

observer's final view on the oscillation power spectrum. This also implies that the code for ray-tracing calculation on virtual observation must be time-dependent.

In order to roughly demonstrate the effective blocking, we calculate the light-curves without the radiation contribution from different inner cutting regions for the same model S8 and we show the relevant power spectra in figure 4. It is remarkable that the fundamental harmonic (inside the rectangle in all four panels) cannot be easily removed from PSDs because of the outward propagation of the oscillation from sonic-point. It implies that the measurement of BH spin with HFQPO will be very robust even in a case when modulation of the innermost disk is not visible.

So far, we have found some features of our model fortunately coinciding with the counterparts of HFQPO observations. All of these are only due to the adopting of a special evolutionary stress equation in our model, which mimics the viscous features induced from MHD simulations. However, our model still lacks some abilities for capturing various complicated features associated with the real accretion flows around BHs. In fact, it is almost impossible for seeing the oscillations during the whole outburst state (like those in figure 1) in real accretion flows. It is because the effective α and viscous time-delay, determining the appearance of oscillations, is turbulent stochastic in real accretion flows though their expected values can be determined by certain laws. Further more MHD simulations on the mean behaviors of effective turbulent viscosity is necessary for improving our understanding on accretion process around BHs (e.g. Hirose et al 2009, 2014; Penna et al 2013). It is also impossible for capturing the resonance between the radial and vertical oscillations suggested by Kluźniak et al (2004), because our model is a vertically integrated model and there is only radial dependence reserved. The further analytic works and MHD simulations on the roles of radial and vertical oscillations are necessary for explaining the observational HFQPO pairs though our model has the intrinsic multi-frequency feature. In fact, the thermal instability required by our model is the theoretical one whose deviations from the observations have been found a decade ago (Gierlinński & Done 2004). While the existence of thermal instability on the BH accretion disks is still an open issue at present, we only can adopt this theoretical thermal instability to produce the high luminosity outburst required by the oscillations in our model. We believe the plausibility of oscillations observed on our models though it is "dancing" on a poor-quality stage.

This work was supported by the National Natural Science Foundation of China under grants 11233006 and 11373002, Polish NCN grant UMO-2011/01/B/ST9/05439 and 2013/08/A/ST9/00795, and Czech ASCRM100031242 CZ.1.07/2.3.00/20.0071 Synergy (Opava) project.

REFERENCES

- Belloni, T. M., Sanna, A., Méndez, M., 2012, MNRAS, 426, 1701
- Chen, X.-M., & Taam, R. E. 1995, ApJ, 441, 354
- Ciesielski, A., Wielgus, M., Kluźniak, W., Sadowski, A., Abramowicz, M., Lasota, J.-P., & Rebusco, P. 2012, A&A, 538, 148
- Gierlinński, M. & Done, C. 2004, MNRAS, 347, 885
- Giussani, L., Kluźniak, W., & Mishra, B. 2014, in Proceedings of RAGtime 16, eds. S. Hledík and Z. Stuchlík,
- Hirose, S., Blaes, O., Krolik, J. H., Coleman, M. S. B., & Sano, T. 2014, ApJ, 787, 1
- Hirose, S., Krolik, J. H., Blaes, O. 2009, ApJ, 691, 16
- Kato, S. 1978, MNRAS, 185, 629
- Kato, S. 2001, PASJ, 53, 1
- Kato, S., Fukue, J., & Mineshige, S. 2008, Black-Hole Accretion Disks: Towards a New Paradigm (Kyoto: Kyoto Univ. Press)
- Kato, S., Honma, F., & Matsumoto, R. 1988, MNRAS, 231, 37
- Kluźniak, W., Abramowicz, M. A., Kato, S., Lee, W. H., & Stergioulas, N. 2004, ApJ, 603, 89
- Lin, D.-B., Gu, W.-M., & Lu, J.-F. 2011, MNRAS, 415, 2319
- Matsumoto R., Kato S., Honma F. 1988, Physics of Neutron Stars and Black Holes, ed Y. Tanaka (Universal Academy Press, Tokyo), p.155
- Matsumoto R., Kato S., Honma F. 1989, Theory of Accretion Disks, ed F. Meyer, W.J. Duschl, J. Frank, E. Meyer-Hofmeister (Kluwer Academic Publisher, Dordrecht), p.167
- Milsom, J. A., Chen, X. M., & Taam, R. E. 1994, ApJ, 421, 668
- Miranda, R., Horák, J., & Lai, D. 2014, arXiv:1408.0800v1
- Penna, R. F., Sądowski, A., Kulkarni, A. K., Narayan, R. 2013, MNRAS, 428, 2255

Remillard, R. A., & McClintock, J. E., 2006, *ARA&A*, 44, 49

Shakura, N. I., & Sunyaev, R. A. 1973, *A&A*, 24, 337

Xue, L., Sądowski, A., Abramowicz, M. A., & Lu, J.-F. 2011, *ApJS*, 195, 7

Yamasaki, T., & Kato, S. 1996, *PASJ*, 48, 99

Table 1. Model Sequences

ID	n	α	M/M_{\odot}	a/M	$\dot{M}/\dot{M}_{\text{Edd}}^1$	Fundamental Frequency [Hz]	Max Epicyclic Frequency [Hz]
S8	1	Eq. (12)	10	0	0.06	71.64-76.73 ²	71.3
S15	1	0.1	10	0	0.06	No Osci.	71.3
S5	1	0.15	10	0	0.06	No Osci.	71.3
S7	1	0.3	10	0	0.06	62.37-68.7	71.3
S4	0	0.3	10	0	0.06	No Osci.	71.3
S3	0	0.45	10	0	0.06	No Osci.	71.3
S16	0	Eq. (12)	10	0	0.06	No Osci.	71.3
S2	0.5	Eq. (12)	10	0	0.06	74.77-80.64 (AD) ³	71.3
S17	0.75	Eq. (12)	10	0	0.06	74.27-78.5 (AD)	71.3
S1	2	Eq. (12)	10	0	0.06	69.77-71 (P)	71.3
S30	4	Eq. (12)	7.02	0.947	0.06	285.64 ⁴	300

¹Eddington accretion rate $\dot{M}_{\text{Edd}} \equiv \frac{64\pi GM}{c\kappa_{\text{es}}} = 2.23 \times 10^8 \frac{M}{M_{\odot}} (\text{gs}^{-1})$.

²The variation range of observed fundamental frequencies is given.

³The characters inside the parentheses denote the luminosity stages in which the oscillations disappear. For example, (AD) denotes the oscillations only appear in the luminosity *plateau* stage (disappear in *ascending* and *descending* stages).

⁴We only have the data for the luminosity ascending stage. Due to the lack of data, we cannot observe any remarkable variance on its fundamental frequency.

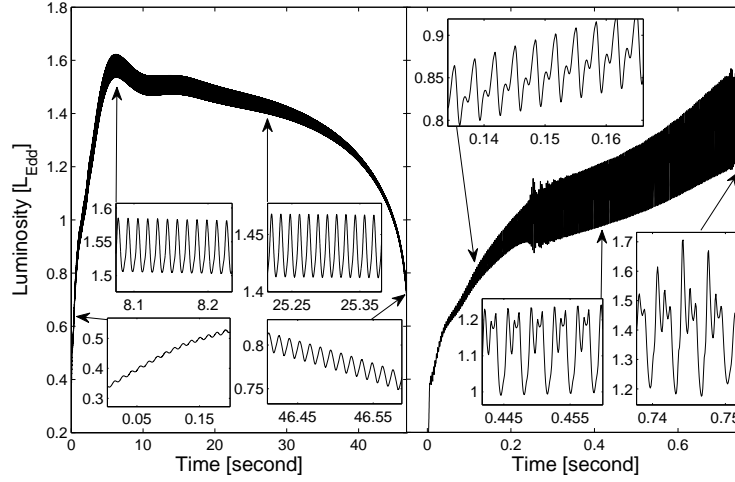


Fig. 1.— Light-curves of models S8 (left) and S30 (right). There are a few subplots to reveal detailed views of surrounding arrow points.

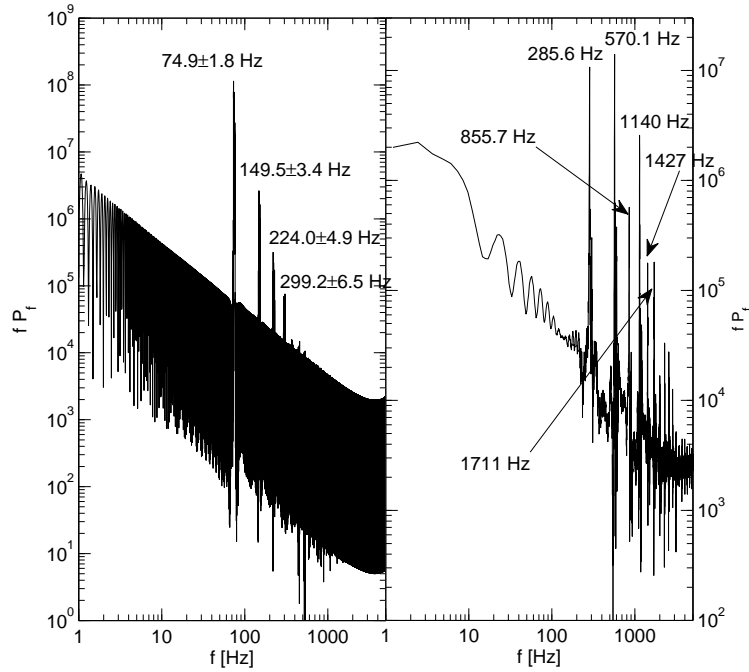


Fig. 2.— PSDs of models S8 (left) and S30 (right).

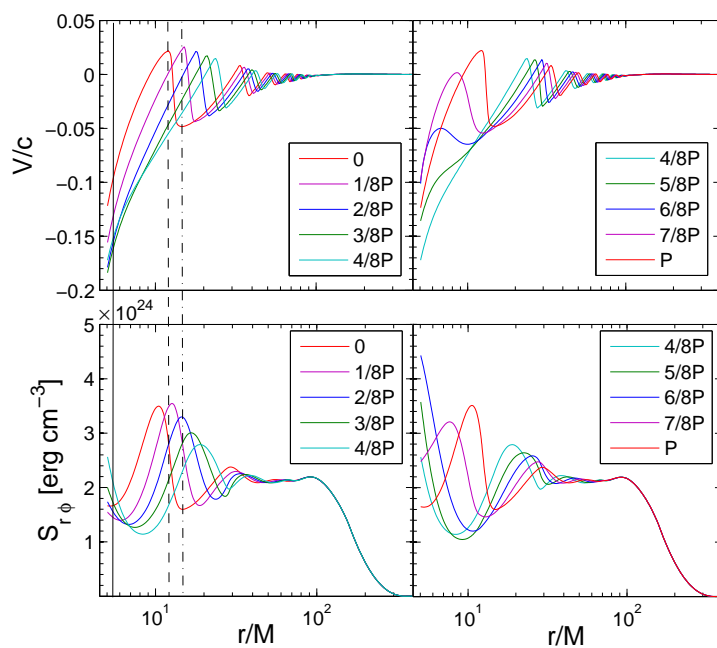


Fig. 3.— One oscillation cycle of the radial velocity and viscous stress from model S8. The different color lines denote a serial snapshotting times, which are all scaled with the period of this cycle. The radius r is scaled with BH mass M because we take $G = c = 1$. Thus the Schwarzschild radius is $2M$.

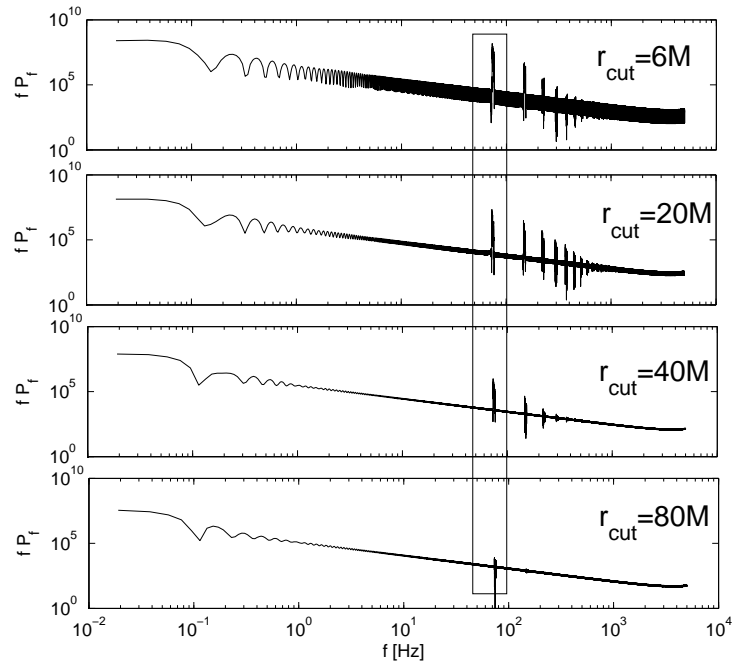


Fig. 4.— PSDs of different blocking cases. From upper to lower, the radii of cutting regions r_{cut} increase for the same model S8.